

RUP-19-16
December, 2019

Quarks mass function at finite density in real-time formalism

Hidekazu TANAKA and Shuji SASAGAWA

Department of Physics, Rikkyo University, Tokyo 171-8501, Japan

ABSTRACT

Chiral symmetry restoration of quarks is investigated at finite density in quantum chromodynamics. The effective quark mass is calculated with the Schwinger-Dyson equation in the real-time formalism without the instantaneous exchange approximation. We present some properties of the quark mass functions and the quark propagator at zero temperature.

§1. Introduction

Evaluation of chiral phase transitions at finite density in quantum chromodynamics (QCD) is difficult task. In order to study the chiral phase transitions, one of useful tools is the Schwinger-Dyson equation (SDE)[1,2], which can evaluate non-perturbative phenomena.

In the previous papers[3,4,5], we formulated the SDE in the real-time formalism (RTF) for QED and QCD without the instantaneous exchange approximation (IEA)[6]. The RTF, which is formulated in Minkowski space, can evaluate non-equilibrium systems. In our method, the resonance contributions in momentum integration in Minkowski space are efficiently evaluated.

In Ref.[5], we found that the critical temperature T_C , in which the chiral symmetry is restored at zero chemical potential, is $T_C \simeq \Lambda_{\text{QCD}}/2$. Furthermore, the effective quark mass evaluated at the resonance peak of an effective quark propagator is given as $M_q \simeq \Lambda_{\text{QCD}}$. Here Λ_{QCD} denotes the QCD scale parameter. Therefore, $\Lambda_{\text{QCD}} \simeq 0.32\text{GeV}$ gives reasonable result for the effective quark mass as well as the critical temperature for the chiral phase transition.

In this paper, we study properties of the quark mass function with the SDE in the RTF beyond the IEA for finite density at zero temperature, which corresponds to a high density matter at low temperature, such as internal structure of neutron stars.

In section 2, we present formula for the SDE in the RTF without the IEA. In section 3, some numerical results for the effective quark mass are calculated. In order to investigate instability of the massive quark state, we evaluate time dependences of the effective quark propagator. Section 4 is devoted to the summary and some comments.

§2. SDE for quark mass function

In the RTF, we implement two types of fields specified by 1 and 2 in the theory. The type-1 field is the usual field and the type-2 field corresponds to a ghost field in the heat bath.

In one-loop order, we calculate the 1-1 component of a self-energy of quark $\Sigma^{11}(P)$ in QCD, which is given by

$$-i\Sigma^{11}(P) = (ig_s)^2 C_F \int \frac{d^4q}{(2\pi)^4} \gamma^\mu iS^{11}(Q) \Gamma^\nu iD_{\mu\nu}^{11}(K), \quad (2.1)$$

where $S^{11}(Q)$ and $D_{\mu\nu}^{11}(K)$ are the 1-1 components of thermal propagators for a quark with momentum $Q = (q_0, \mathbf{q})$ and a gluon with momentum $K = P - Q = (k_0, \mathbf{k})$, respectively. An external momentum of the quark is denoted by $P = (p_0, \mathbf{p})$. In our formulation, the time evolution of the system is generated with an operator $\hat{H}' = \hat{H} - \mu\hat{N}$. Here \hat{H} and \hat{N} denote a hamiltonian and a number operator of the quark, respectively. The energy eigenvalues for \hat{H}' are denoted by p_0 and q_0 . In our calculation, the quark-gluon vertex is defined by $\Gamma^\nu = \gamma^\nu$ with the gamma matrices γ^ν . The strong coupling constant and the color factor are denoted by g_s

and $C_F = 4/3$, respectively.

The 1-1 component of the quark propagator in the RTF is given as

$$iS^{11}(Q) = i[(S_F(Q))_R + i(S_F(Q))_I N_F(\mu, q_0)], \quad (2.2)$$

where $N_F(\mu, q_0) = \epsilon(q_0 + \mu)\epsilon(q_0)$ with a chemical potential μ at zero temperature, in which we define $\epsilon(z) = \theta(z) - \theta(-z)$ with the step function $\theta(z)$. Here, $(S_F(Q))_R$ and $(S_F(Q))_I$ are the real and imaginary parts of the quark propagator $S_F(Q)$, respectively. The quark propagator $S_F(Q)$ is defined as

$$iS_F(Q) \equiv i(\not{Q} + \gamma^0 \mu + M(Q))I_F(Q). \quad (2.3)$$

with

$$I_F(Q) = \frac{1}{(q_0 + \mu)^2 - \mathbf{q}^2 - M^2(Q) + i\varepsilon}. \quad (2.4)$$

The 1-1 component of the gluon propagator is given as

$$iD_{\mu\nu}^{11}(K) = iD_{F\mu\nu}(K) = i[(D_{F\mu\nu}(K))_R + i(D_{F\mu\nu}(K))_I], \quad (2.5)$$

where

$$iD_{F\mu\nu}(K) \equiv P_{\mu\nu}^L iD_L(K) + P_{\mu\nu}^T iD_T(K) \quad (2.6)$$

with

$$P_{\mu\nu}^L = -g_{\mu\nu} + \frac{K_\mu K_\nu}{K^2} - P_{\mu\nu}^T \quad (2.7)$$

and

$$P_{\mu\nu}^T = \left(-g_{\mu\nu} + \frac{K_\mu K_\nu}{\mathbf{k}^2}\right)(1 - \delta_{0\mu})(1 - \delta_{0\nu}), \quad (2.8)$$

where the longitudinal and transverse components of the gluon propagator are given as

$$iD_L(K) = \frac{i}{K^2 - m_L^2 + i\varepsilon} \quad (2.9)$$

and

$$iD_T(K) = \frac{i}{K^2 - m_T^2 + i\varepsilon}, \quad (2.10)$$

respectively. Here, m_L and m_T denote the longitudinal and transverse gluon masses, respectively.

Integrating over the azimuthal angle of the quark momentum \mathbf{q} , the trace of the self-energy Σ^{11} is given by

$$M^{11}(P) \equiv \frac{1}{4}Tr[\Sigma^{11}(P)] = -\frac{iC_F}{2\pi^2} \int_{-A_0}^{A_0} dq_0 \int_{\delta}^A dq \frac{q}{p} \alpha_s [MI_{11}J_{11}](P, Q) \quad (2.11)$$

with $p = |\mathbf{p}|, q = |\mathbf{q}|$, and $\alpha_s = g_s^2/(4\pi)$, ^{*)} where,

$$MI_{11} = (MI_F)_R + i(MI_F)_I N_F(\mu, q_0) \quad (2.12)$$

and

$$J_{11} = (J_F)_R + i(J_F)_I. \quad (2.13)$$

with

$$J_F = \int_{\eta_-}^{\eta_+} dk k [D_L(K) + 2D_T(K)] \quad (2.14)$$

with $\eta_{\pm} = |p \pm q|$ and $k = |\mathbf{k}|$, respectively.

The real part M_R and the imaginary part M_I of the mass M in Eq.(2.3) are given by $M_R = (M^{11})_R$ and $M_I = (M^{11})_I/N_F(\mu, q_0)$, respectively. On the other hand, the real part $(M^2)_R$ and the imaginary part $(M^2)_I$ of the mass M^2 in Eq.(2.4) are given by $(M^2)_R = (M_R)^2 - (M_I)^2$ and $(M^2)_I = 2M_R M_I$, respectively.

In Minkowski space, if the imaginary part of the mass function $(M^2)_I$ is small, the quark propagator I_F in Eq.(2.4) varies rapidly near $(q_0 + \mu)^2 - q^2 \simeq (M^2)_R$. As implemented in the previous works [4,5,6], we divide the q_0 integration into small ranges and integrate the quark propagator over $q_0^{(l)} \leq q_0 \leq q_0^{(l+1)}$ ($q_0^{(1)} = -\Lambda_0, q_0^{(N)} = \Lambda_0$), in which remaining contributions of the integrand are averaged over the range $q_0^{(l)} \leq q_0 \leq q_0^{(l+1)}$.

In order to investigate instability of the massive quark state, we evaluate time dependences of the quark propagator

$$i\tilde{S}_F(x_0, \mathbf{p}) = \int d^3x iS_F(x_0, \mathbf{x}) e^{-i\mathbf{x} \cdot \mathbf{p}} \quad (2.15)$$

with

$$iS_F(x_0, \mathbf{x}) = \int \frac{d^4Q}{(2\pi)^4} iS_F(Q) e^{-i(x_0 q_0 - \mathbf{x} \cdot \mathbf{q})}, \quad (2.16)$$

where x_0 and \mathbf{x} denote a time and a space coordinates, respectively.

Integrating over \mathbf{q} , the quark propagator $i\tilde{S}_F(x_0, \mathbf{p})$ is given as

$$i\tilde{S}_F(x_0, \mathbf{p}) = \int \frac{dq_0}{2\pi} iS_F(\tilde{Q}) e^{-ix_0 q_0} \quad (2.17)$$

with $\tilde{Q} = (q_0, \mathbf{p})$. We separate $i\tilde{S}_F(x_0, \mathbf{p})$ as

$$i\tilde{S}_F(x_0, \mathbf{p}) = i\tilde{S}_F^{(+)}(x_0, \mathbf{p}) + i\tilde{S}_F^{(-)}(x_0, \mathbf{p}) \quad (2.18)$$

with

$$i\tilde{S}_F^{(\pm)}(x_0, \mathbf{p}) = \pm \int \frac{dq_0}{2\pi} \frac{i(\tilde{Q} + \gamma^0 \mu + M(\tilde{Q}))}{(q_0 + \mu) \mp E(\tilde{Q})} \frac{1}{2E(\tilde{Q})} e^{-ix_0 q_0}, \quad (2.19)$$

^{*)} In numerical calculations, the strong coupling constant α_s is replaced by the running coupling constant $\alpha_s(t) = g_s^2(t)/(4\pi)$ [7] with $t = \log[(\bar{P}^2 + \bar{Q}^2 + \mu^2)/\Lambda_{\text{QCD}}^2]$, where $\bar{P}^2 = p_0^2 + p^2$ and $\bar{Q}^2 = q_0^2 + q^2$.

where E is the quark energy. The real and imaginary parts of the quark energy E_R and E_I are defined by $E_R = |E| \cos(\Phi/2)$ and $E_I = |E| \sin(\Phi/2)$ with $\Phi = \arctan((E^2)_I/(E^2)_R)$ and $|E| = \sqrt{|E^2|} = ((E^2)_R^2 + (E^2)_I^2)^{1/4}$. Here the real and imaginary parts of the squared quark energy E^2 are defined as $(E^2)_R = \mathbf{p}^2 + (M^2)_R$ and $(E^2)_I = (M^2)_I - \varepsilon$, respectively.

Here, $i\tilde{S}_F^{(\pm)}$ are further written by

$$i\tilde{S}_F^{(\pm)}(x_0, \mathbf{p}) = \pm i\gamma_0 \int \frac{dq_0}{2\pi} \frac{1}{2E(\tilde{Q})} e^{-ix_0 q_0} + i\bar{S}_F^{(\pm)}(x_0, \mathbf{p}) \quad (2.20)$$

with

$$i\bar{S}_F^{(\pm)}(x_0, \mathbf{p}) = \pm \int \frac{dq_0}{2\pi} \frac{i(\bar{Q}_\pm + M(\tilde{Q}))}{(q_0 + \mu) \mp E(\tilde{Q})} \frac{1}{2E(\tilde{Q})} e^{-ix_0 q_0}, \quad (2.21)$$

where $\bar{Q}_\pm = (\pm E, \mathbf{p})$. Here the first terms in Eq.(2.20) are canceled in $i\tilde{S}_F(x_0, \mathbf{p})$.

Using

$$\frac{1}{(q_0 + \mu) - E(\tilde{Q})} e^{-ix_0 q_0} = -i \int_{-\infty}^{x_0} dy_0 e^{-iq_0 y_0 - i(E(\tilde{Q}) - \mu)(x_0 - y_0)} \quad (2.22)$$

for $E_I < 0$ and

$$\frac{1}{(q_0 + \mu) - E(\tilde{Q})} e^{-ix_0 q_0} = i \int_{x_0}^{\infty} dy_0 e^{-iq_0 y_0 - i(E(\tilde{Q}) - \mu)(x_0 - y_0)} \quad (2.23)$$

for $E_I > 0$, the quark propagator $i\tilde{S}_F^{(+)}(x_0, \mathbf{p})$ is given as

$$i\tilde{S}_F^{(+)}(x_0, \mathbf{p}) = \int \frac{dq_0}{2\pi} \int_{-\infty}^{x_0} dy_0 \frac{(\bar{Q}_+ + M(\tilde{Q}))}{2E(\tilde{Q})} e^{-iy_0 q_0 - i(E(\tilde{Q}) - \mu)(x_0 - y_0)} \quad (2.24)$$

for $E_I < 0$ and

$$i\tilde{S}_F^{(+)}(x_0, \mathbf{p}) = - \int \frac{dq_0}{2\pi} \int_{x_0}^{\infty} dy_0 \frac{(\bar{Q}_+ + M(\tilde{Q}))}{2E(\tilde{Q})} e^{-iy_0 q_0 - i(E(\tilde{Q}) - \mu)(x_0 - y_0)} \quad (2.25)$$

for $E_I > 0$, respectively.

Similarly using

$$\frac{1}{(q_0 + \mu) + E(\tilde{Q})} e^{-ix_0 q_0} = i \int_{x_0}^{\infty} dy_0 e^{-iq_0 y_0 + i(E(\tilde{Q}) + \mu)(x_0 - y_0)} \quad (2.26)$$

for $E_I < 0$ and

$$\frac{1}{(q_0 + \mu) + E(\tilde{Q})} e^{-ix_0 q_0} = -i \int_{-\infty}^{x_0} dy_0 e^{-iq_0 y_0 + i(E(\tilde{Q}) + \mu)(x_0 - y_0)} \quad (2.27)$$

for $E_I > 0$, the quark propagator $i\tilde{S}_F^{(-)}(x_0, \mathbf{p})$ is given as

$$i\tilde{S}_F^{(-)}(x_0, \mathbf{p}) = \int \frac{dq_0}{2\pi} \int_{x_0}^{\infty} dy_0 \frac{(\bar{Q}_- + M(\tilde{Q}))}{2E(\tilde{Q})} e^{-iy_0 q_0 + i(E(\tilde{Q}) + \mu)(x_0 - y_0)} \quad (2.28)$$

for $E_I < 0$ and

$$i\bar{S}_F^{(-)}(x_0, \mathbf{p}) = - \int \frac{dq_0}{2\pi} \int_{-\infty}^{x_0} dy_0 \frac{(\bar{Q} - + M(\tilde{Q}))}{2E(\tilde{Q})} e^{-iy_0 q_0 + i(E(\tilde{Q}) + \mu)(x_0 - y_0)} \quad (2.29)$$

for $E_I > 0$, respectively.

§3. Numerical results

In this section, some numerical results are presented. We solve the SDE presented in Eq. (2.11) by a recursion method starting from a constant mass at $\mu = 0$. *)

For each iteration, the mass function is normalized by a current quark mass at large $\zeta^2 = p_0^2 - p^2$, in which perturbative calculations are reliable.

In the iteration, the mass function $M(p_0, p)$ in integrand of the SDE is replaced by the renormalized one obtained by the previous iteration. **)

In this paper, we evaluate integrated mass functions $\langle |M| \rangle$, $\langle M_R \rangle$ and $\langle M_I \rangle$ as order parameters, in which $|M(p_0, p)|$, $M_R(p_0, p)$ and $M_I(p_0, p)$ are integrated over p_0 and p , respectively.[5]

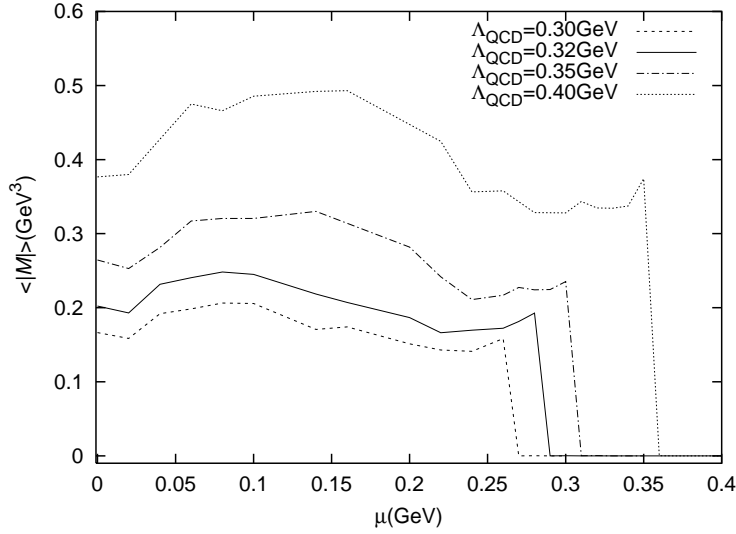


Fig. 1. The μ dependences of the integrated quark mass functions $\langle |M| \rangle$ with $\Lambda_{\text{QCD}} = 0.30 \text{ GeV}, 0.32 \text{ GeV}, 0.35 \text{ GeV}$ and 0.40 GeV , respectively, with the massless gluon.

In Fig.1, the μ dependences of $\langle |M| \rangle$ for $\Lambda_{\text{QCD}} = 0.30 \text{ GeV}, 0.32 \text{ GeV}, 0.35 \text{ GeV}$ and 0.40 GeV with the massless gluon are presented at $T = 0$. The transition of the chiral symmetry restoration seems to be the first order. The critical chemical

*) The initial input parameters are $M_R = \Lambda_{\text{QCD}}$ and $M_I = 0$ at $\mu = 0$ with $\Lambda_0 = \Lambda = 10\Lambda_{\text{QCD}}$ and $\delta = 0.1\Lambda_{\text{QCD}}$ with $\varepsilon = 10^{-6}$. In evaluation of the quark mass function at $\mu + \Delta\mu$, we implement the solution of M obtained at μ as the initial input.

**) We take the renormalized mass $m(\zeta^2) = 0$ at $\zeta = 10\Lambda_{\text{QCD}}$.

potential of the phase transition μ_C depends on the QCD parameter Λ_{QCD} . In our calculation, $0.30 \text{ GeV} \leq \Lambda_{\text{QCD}} \leq 0.40 \text{ GeV}$ gives $0.27 \text{ GeV} \leq \mu_C \leq 0.36 \text{ GeV}$, roughly $\mu_C \sim 0.9\Lambda_{\text{QCD}}$.

In order to choose the QCD parameter Λ_{QCD} , we need another condition. Our model roughly gives the real part of the squared quark mass function $(M^2)_R \simeq \Lambda_{\text{QCD}}^2$ at $\mu = T = 0$. Here, $(M^2)_R$ is determined by the resonance peak of the quark propagator. In our calculation, $\Lambda_{\text{QCD}} = 0.32 \text{ GeV}$ gives $\sqrt{(M^2)_R} \simeq 0.32 \text{ GeV}$ at $T = \mu = 0$ and the critical temperature of the chiral symmetry restoration $T_C \simeq 0.175 \text{ GeV}$ with $\mu = 0$. [5]

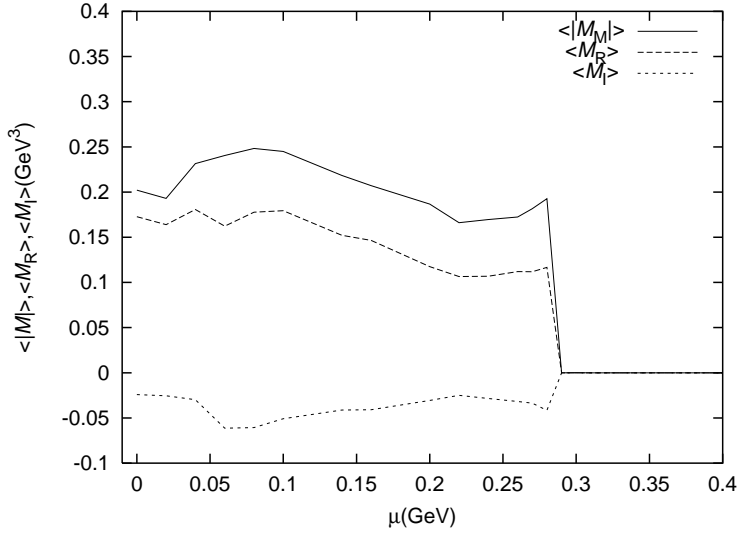


Fig. 2. The μ dependences of the integrated quark mass functions $\langle |M| \rangle$, $\langle M_R \rangle$ and $\langle M_I \rangle$ at $\Lambda_{\text{QCD}} = 0.32 \text{ GeV}$ with the massless gluon.

In Fig.2, the μ dependences of the integrated quark mass functions $\langle |M| \rangle$, $\langle M_R \rangle$ and $\langle M_I \rangle$ with the massless gluon are presented at $\Lambda_{\text{QCD}} = 0.32 \text{ GeV}$, which gives $\mu_C \simeq 0.29 \text{ GeV}$.

As shown in Fig.2, the imaginary part of the mass function $\langle M_I \rangle$ is non-zero value for broken chiral symmetric phase below the critical chemical potential μ_C , which means the massive quark state may be unstable if energy scale rapidly changes. Furthermore, the real and imaginary parts vanish at the same critical chemical potential.

In order to investigate instability of the massive quark state, we calculate a time dependence of the quark propagator $i\bar{S}_F^{(+)}(x_0, \mathbf{p})$ in Eq.(2·21), which is separated as

$$i\bar{S}_F^{(+)}(x_0, \mathbf{p}) = \gamma_\mu iS_+^\mu(x_0, \mathbf{p}) + iS_+^M(x_0, \mathbf{p}) \quad (3.1)$$

with

$$iS_+^\mu(x_0, \mathbf{p}) = i \int \frac{dq_0}{2\pi} \frac{\bar{Q}_+^\mu}{(q_0 + \mu) - E(q_0, p)} \frac{1}{2E(q_0, p)} e^{-ix_0 q_0} \quad (3.2)$$

and

$$iS_+^M(x_0, \mathbf{p}) = i \int \frac{dq_0}{2\pi} \frac{M(q_0, p)}{(q_0 + \mu) - E(q_0, p)} \frac{1}{2E(q_0, p)} e^{-ix_0 q_0}. \quad (3.3)$$

From Eqs.(2.24) and (2.25), the real and imaginary parts of $iS_+^\mu(x_0, \mathbf{p})$ and $iS_+^M(x_0, \mathbf{p})$ are given as

$$\begin{aligned} \text{Re} [iS_+^\mu(x_0, \mathbf{p})] &= \int_{-x_M}^{x_0} dy_0 \int_{-\Lambda_0}^{\Lambda_0} \frac{dq_0}{2\pi} \frac{|\bar{Q}_+^\mu|}{2|E(q_0, p)|} \cos(\Psi^\mu) e^{E_I(q_0, p)(x_0 - y_0)} \theta(-E_I(q_0, p)) \\ &\quad - \int_{x_0}^{x_M} dy_0 \int_{-\Lambda_0}^{\Lambda_0} \frac{dq_0}{2\pi} \frac{|\bar{Q}_+^\mu|}{2|E(q_0, p)|} \cos(\Psi^\mu) e^{E_I(q_0, p)(x_0 - y_0)} \theta(E_I(q_0, p)) \end{aligned} \quad (3.4)$$

and

$$\begin{aligned} \text{Im} [iS_+^\mu(x_0, \mathbf{p})] &= - \int_{-x_M}^{x_0} dy_0 \int_{-\Lambda_0}^{\Lambda_0} \frac{dq_0}{2\pi} \frac{|\bar{Q}_+^\mu|}{2|E(q_0, p)|} \sin(\Psi^\mu) e^{E_I(q_0, p)(x_0 - y_0)} \theta(-E_I(q_0, p)) \\ &\quad + \int_{x_0}^{x_M} dy_0 \int_{-\Lambda_0}^{\Lambda_0} \frac{dq_0}{2\pi} \frac{|\bar{Q}_+^\mu|}{2|E(q_0, p)|} \sin(\Psi^\mu) e^{E_I(q_0, p)(x_0 - y_0)} \theta(E_I(q_0, p)), \end{aligned} \quad (3.5)$$

with

$$\Psi^\mu = q_0 y_0 + (E_R(q_0, p) - \mu)(x_0 - y_0) + \Phi_Q^\mu - \Phi/2 \quad (3.6)$$

for $iS_+^\mu(x_0, \mathbf{p})$, and

$$\begin{aligned} \text{Re} [iS_+^M(x_0, \mathbf{p})] &= \int_{-x_M}^{x_0} dy_0 \int_{-\Lambda_0}^{\Lambda_0} \frac{dq_0}{2\pi} \frac{|M(q_0, p)|}{2|E(q_0, p)|} \cos(\Psi^M) e^{E_I(q_0, p)(x_0 - y_0)} \theta(-E_I(q_0, p)) \\ &\quad - \int_{x_0}^{x_M} dy_0 \int_{-\Lambda_0}^{\Lambda_0} \frac{dq_0}{2\pi} \frac{|M(q_0, p)|}{2|E(q_0, p)|} \cos(\Psi^M) e^{E_I(q_0, p)(x_0 - y_0)} \theta(E_I(q_0, p)) \end{aligned} \quad (3.7)$$

and

$$\begin{aligned} \text{Im} [iS_+^M(x_0, \mathbf{p})] &= - \int_{-x_M}^{x_0} dy_0 \int_{-\Lambda_0}^{\Lambda_0} \frac{dq_0}{2\pi} \frac{|M(q_0, p)|}{2|E(q_0, p)|} \sin(\Psi^M) e^{E_I(q_0, p)(x_0 - y_0)} \theta(-E_I(q_0, p)) \\ &\quad + \int_{x_0}^{x_M} dy_0 \int_{-\Lambda_0}^{\Lambda_0} \frac{dq_0}{2\pi} \frac{|M(q_0, p)|}{2|E(q_0, p)|} \sin(\Psi^M) e^{E_I(q_0, p)(x_0 - y_0)} \theta(E_I(q_0, p)), \end{aligned} \quad (3.8)$$

with

$$\Psi^M = q_0 y_0 + (E_R(q_0, p) - \mu)(x_0 - y_0) + \Phi_M - \Phi/2 \quad (3.9)$$

for $iS_+^M(x_0, \mathbf{p})$, respectively.*) Here, Φ_Q^μ and Φ_M are defined as

$$\Phi_Q^0 = \Phi/2 \quad (3.10)$$

and

$$\Phi_Q^i = \pi\theta(-p^i) \quad (3.11)$$

for $i = 1, 2, 3$, and

$$\Phi_M = \arctan \frac{M_I}{M_R}, \quad (3.12)$$

respectively. In our calculations, we set the momentum \mathbf{p} as $\mathbf{p} = (p^1, p^2, p^3) = (0, 0, p)$

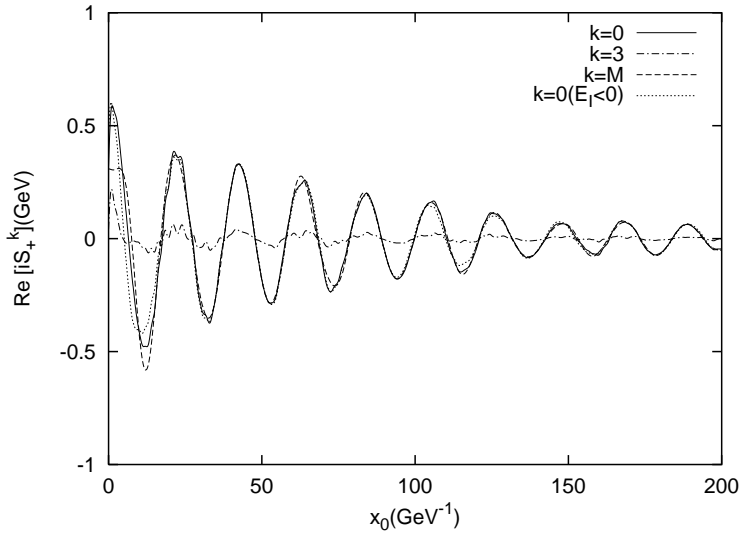


Fig. 3. The x_0 dependences of the quark propagator $\text{Re}[iS_+^k(x_0, \delta)]$ with $\mu = 0.0$ GeV and $p = \delta = 0.1\Lambda_{\text{QCD}}$ for $k = 0, 3, M$, respectively, at $\Lambda_{\text{QCD}} = 0.32$ GeV with the massless gluon. The dotted curve denotes the quark propagator $\text{Re}[iS_0(x_0, \delta)]$ for $E_I < 0$

In Fig.3, the real part of $iS_+^k(x_0, \mathbf{p})$ with $p = \delta = 0.1\Lambda_{\text{QCD}}$ for $k = 0, 3, M$, respectively, are presented at $\Lambda_{\text{QCD}} = 0.32$ GeV and $\mu = 0.0$ GeV with the massless gluon. We can see that $iS_+^0(x_0, \delta) \simeq iS_+^M(x_0, \delta) \gg iS_+^3(x_0, \delta)$, since $|E| \simeq |M| \gg \delta$. As shown in Fig.3, the amplitude of the quark propagator decreases as increasing x_0 , which means the imaginary part of the quark energy E_I plays a role of decay constant. The dotted curve denotes the quark propagator $\text{Re}[iS_+^M(x_0, \delta)]$ for $E_I < 0$. Therefore, the contribution from $E_I > 0$ is not significant for the time evolution of the quark propagator.

In Fig.4, the x_0 dependences of the quark propagator $\text{Re}[iS_+^0(x_0, \delta)]$ for $\mu = 0.0$ GeV, 0.1 GeV and 0.2 GeV, respectively, are presented at $\Lambda_{\text{QCD}} = 0.32$ GeV with the massless gluon. As shown in Fig.4, the wavelength is longer as μ increases due to the term $(E_R - \mu)x_0$ of the phase Ψ^0 in Eq.(3.6).

*) x_M is taken as $x_M = 10x_{\text{max}}$. Here, x_{max} is an maximum value of the plot for x_0 .

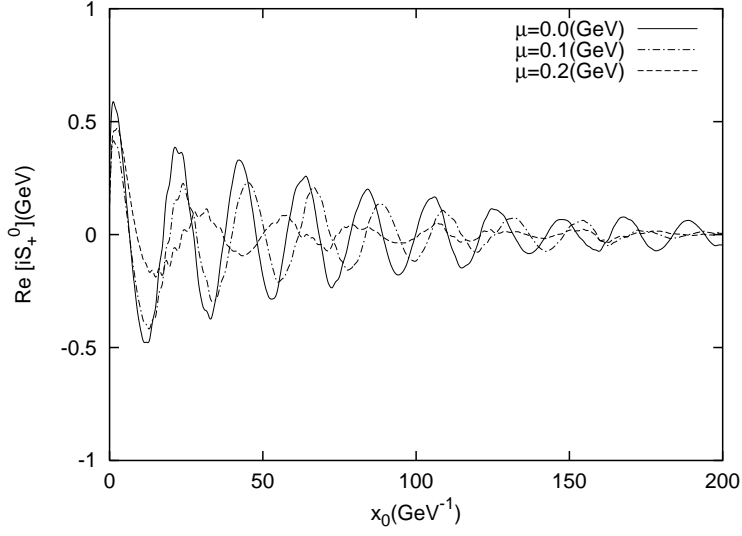


Fig. 4. The x_0 dependences of the quark propagator $\text{Re}[iS_+^0(x_0, \delta)]$ for $\mu = 0.0$ GeV, 0.1 GeV and 0.2 GeV, respectively, at $\Lambda_{\text{QCD}} = 0.32$ GeV with the massless gluon.

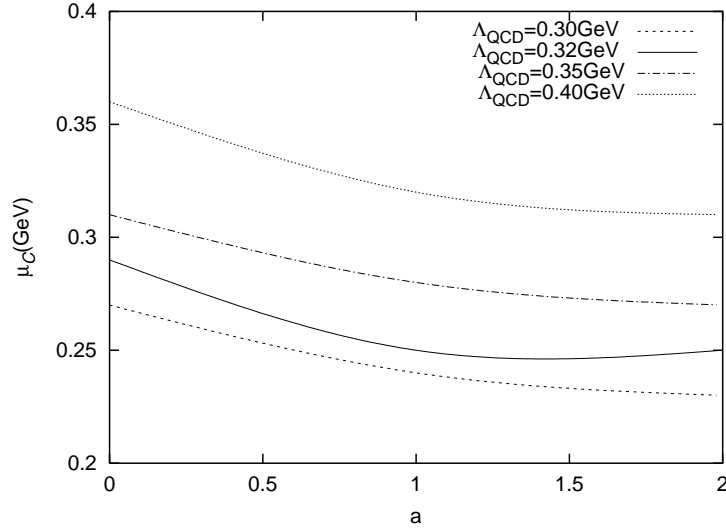


Fig. 5. The a dependences on μ_C with the gluon masses defined by $m_T = 0$ and $m_L = a\Lambda_{\text{QCD}}$ with $\Lambda_{\text{QCD}} = 0.30$ GeV, 0.32 GeV, 0.35 GeV and 0.40 GeV, respectively.

In Fig.5, the gluon mass dependences are presented for different values of Λ_{QCD} with $\Lambda_{\text{QCD}} = 0.30$ GeV, 0.32 GeV, 0.35 GeV and 0.40 GeV, respectively. The gluon masses are defined as $m_T = 0$ and $m_L = a\Lambda_{\text{QCD}}$ with a parameter a . Though the critical chemical potential μ_C depends on the gluon mass, the gluon mass dependence on the effective quark mass seems to be weaker for larger gluon mass.

§4. Summary and Comments

In this paper, we have investigated quark mass functions solved by the Schwinger-Dyson equation (SDE) at finite density with zero temperature in the real-time formalism (RTF).

In our model, the critical chemical potential μ_C , in which the chiral symmetry is restored, depends on the QCD scale parameter Λ_{QCD} and the gluon masses (m_L and m_T). Here, m_L and m_T denote the masses for a longitudinal component and a transverse component of the gluon propagator, respectively. Our model roughly gives the critical chemical potential for the chiral symmetry restoration $\mu_C \sim 0.9\Lambda_{\text{QCD}}$ at $T = 0$ with a massless gluon ($m_L = m_T = 0$). The transition of the chiral symmetry restoration seems to be the first order at $T = 0$.

We found that the imaginary part of the integrated mass function $\langle M_I \rangle$ is non-zero value for broken chiral symmetric phase, which means that the massive quark state may be unstable for $\mu < \mu_C$. Furthermore, the real and imaginary parts of the integrated mass functions vanish at the same critical point.

In order to examine the effect of the imaginary part of the quark energy E_I , we calculated the time evolution of the quark propagator. The quark propagator decreases as increasing the time, which suggests that main contribution of the imaginary part of the energy comes from $E_I < 0$. The contribution from $E_I > 0$ does not give significant contribution for the time evolution of the quark propagator.

We also calculated the gluon mass dependence of the quark mass function with a simple ansatz. We presented the critical chemical potential with $m_L = a\Lambda_{\text{QCD}}$ for $0 \leq a \leq 2$ and $m_T = 0$ for different values of Λ_{QCD} . Though the critical chemical potential decreases as increasing the gluon mass m_L , the gluon mass dependence is weaker for large m_L .

Further studies are needed for the mass function in entire range of the phase diagram, in order to know behaviors of the quark mass at strong coupling region.

Acknowledgements

This work was partially supported by MEXT-Supported Program for the Strategic Research Foundation at Private Universities, 2014-2017 (S1411024).

References

- 1) F.J.Dyson, Phys.Rev.**75** (1949) ,1736.
- 2) J.S.Schwinger,Proc.Nat.Acad.Sci.**37** (1951),452.
- 3) S.Sasagawa and H.Tanaka, Prog.Theor.Exp.Phys. **2017**,013B04(2017) [arXiv:1602:04291 [hep-ph]].
- 4) H.Tanaka and S.Sasagawa, Prog.Theor.Exp.Phys. **2017**,123B02(2017) [arXiv:1705:09781 [hep-ph]].
- 5) H.Tanaka and S.Sasagawa, Prog.Theor.Exp.Phys. **2019**,033B04(2019) [arXiv:1808:01777 [hep-ph]].
- 6) K.Fukazawa, T.Inagaki, S.Mukaigawa and T.Muta, Prog. Theor. Phys. **105** (2001),979 [arXiv:hep-ph/9910305].
- 7) Y.Taniguchi and Y.Yoshida Phys. Rev. **D55**,2238(1997).